Computers and Chemical Engineering 153 (2021) 107441

Contents lists available at ScienceDirect

Computers and Chemical Engineering

journal homepage: www.elsevier.com/locate/compchemeng

Performance evaluation and boron rejection in a SWRO system under variable operating conditions

A. Ruiz-García*, I. Nuez

Department of Electronic Engineering and Automation, University of Las Palmas de Gran Canaria, Campus Universitario de Tafira, E-35017 Las Palmas de Gran Canaria (Gran Canaria), Spain

ARTICLE INFO

Article history:
Received 16 April 2021
Revised 21 June 2021
Accepted 4 July 2021
Available online 6 July 2021

Keywords:
Desalination
Reverse osmosis
Boron rejection
Variable operation
Renewable energy

ABSTRACT

It is well known that reverse osmosis (RO) is the leading desalination technology. As an energy intensive technology, the exploitation of renewable energy sources (RES) to power RO systems is a attractive option. A strategy to take advantage of all the available energy of an off-grid renewable system is to work with the RO system under variable operating conditions. This implies additional challenges in terms of water production and permeate quality, among others. Boron rejection is one of the main concerns in seawater RO (SWRO) systems. The aim of this work was to evaluate the performance and boron rejection of a single-stage SWRO system with 7 membrane elements per pressure vessel under variable operating conditions. The initial permeability coefficients of two SWRO membranes (TM820L-440 and TM820S-400) were calculated from experimental data of a full-scale SWRO desalination plant. These coefficients and the characteristics of the membranes were introduced in a simulation algorithm to estimate the behavior of the SWRO system. The results show that, compared with the TM820S-400 membrane, the TM820L-440 performed better in terms of boron rejection in the form of boric acid, but worse in terms of water production. When RES-powered SWRO systems are designed to work under variable operating conditions, consideration needs to be given to the safe operation window in terms of boron concentration in the permeate and to variation of the permeability coefficient of the membranes.

1. Introduction

Boron is an important nutrient, especially for plant growth (Darwish et al., 2020). The margin between a deficient and a toxic concentration of boron is very small and the regulations in this respect are therefore usually quite restrictive (Ruiz-García et al., 2019). Usually, boron concentration in seawater is around 5 ppm and is in the form of boric acid (H_3BO_3) (Hilal et al., 2011). This is an uncharged weak acid and the separation of species by reverse osmosis (RO) membranes depends mainly on their charge (Qasim et al., 2019). As a result, boron rejection is a major concern in seawater reverse osmosis (SWRO) desalination plants (Cengeloglu et al., 2008; Koseoglu et al., 2008b). Considerable efforts have been made to make new RO membranes that increase boron rejection (Li et al., 2020; Jung et al., 2020). Another well-developed research line is related to proposals for alternative processes to RO that separate boron from aqueous solutions or seawater (Wolska and Bryjak, 2013; Najid et al., 2021). These processes include adsorption (Kluczka et al., 2019), adsorption-membrane filtration (Darwish et al., 2017), electrocoagulation (Chen et al., 2020), electrodialysis (Jarma et al., 2021), hybrid FO-RO processes (Ban et al., 2019), membrane distillation (Alkhudhiri et al., 2020; Ozbey-Unal et al., 2018), forward osmosis (FO) (Darwish et al., 2020), ion exchange resins (Hussain et al., 2019), polymer-enhanced ultrafiltration (Neo et al., 2019), and continuous electrodeionization (Jiang et al., 2018). Although SWRO desalination technology is able to produce permeate water with appropriate boron concentrations, there is a high degree of dependency on a number of factors, including the membrane boron permeability coefficient (B_B) (Wang et al., 2018), operating conditions (Hyung and Kim, 2006; Sagiv and Semiat, 2004) and the fouling effect during the operating time that can produce an increase in B_B (Ruiz-García et al., 2019). This question becomes more challenging when an RO desalination plant is forced to operate under variable operating conditions (Ruiz-García et al., 2020).

The challenge to reduce boron concentration in the permeate produced by SWRO desalination plants has been studied extensively by the scientific community (Farhat et al., 2013). This is an

* Corresponding author.
E-mail addresses: alejandro.ruiz@ulpgc.es (A. Ruiz-García), ignacio.nuez@ulpgc.es (I. Nuez).

https://doi.org/10.1016/j.compchemeng.2021.107441

Nomenclature

Acronyms

FO	Forward osmosis
PV	Pressure vessel
RES	Renewable energy sources
ROSA	Reverse Osmosis System Analysis
RO	Reverse osmosis
SOW	Safe operation window
SWRO	Seawater reverse osmosis
WAVE	Water Application Value Engine
WHO	World Health Organization
A	Initial water permeability coefficient (m $Pa^{-1}s^{-1}$)
B	Initial ion permeability coefficient (m s^{-1})
C	Concentration (ppm)
FF	Flow factor
h	Feed-brine spacer height (m
J	Flux per unit area (m^3 $m^{-2}s^{-}1$
k	Mass transfer coefficient
L	Membrane length (m)
NDP	Net driven pressure (Pa)
p	Pressure (Pa)
PF	Polarization factor
Q	Flow (m^3 h^{-1})
R	Flux recovery (%)
S_m	Membrane surface (m^2)
Sc	Schmidt number
SEC	Specific energy consumption (k W h $m^{-}3$)
Sh	Sherwood number
T	Temperature (°C)
TCF	Temperature correction factor
TDS	Total dissolved solids (ppm)
Y	Fraction recovery

Greek letters

$\Delta\pi$	Osmotic pressure gradient (Pa)
Δp	Pressure drop (Pa)
η	Dynamic viscosity (kg $m^{-1}s$)
λ	Friction factor
ν	Velocity (m s^{-1})
π	Osmotic pressure (Pa)
ε	Porosity in feed-spacer channel

Subscripts

av	Average
B	Boron
b	Brine
f	Feed
m	Membrane
p	Permeate
s	Solute

important issue not only because high boron concentration could be toxic for human beings but also because it could have adverse effect on flora and fauna if its concentration is above tolerable levels (Glueckstern and Priel, 2003). Boron rejection in SWRO systems depends, among other things, on feedwater pH, boron concentration, salinity and temperature (T_f) and operating parameters such as pressure (p), flux recovery (R) and membrane characteristics (Hyung and Kim, 2006; Koseoglu et al., 2008b). Membrane manufacturers provide information about boron rejection under test conditions which do not reflect the real operating conditions of full-scale desalination plants. Evaluation of the boron rejection of commercial SWRO elements under different conditions is of fundamental importance. Koseoglu et al. (2008a) studied the boron rejection of two commercial high rejection SWRO membranes using a lab-scale flat-sheet configuration. They studied the influence of pH, p and salinity on boron rejection. Increasing the pH can have a positive effect on boron rejection but can also cause scaling problems in RO systems (Hasson et al., 2011). The difficulty that SWRO membranes have to reject boron has caused, in some cases, redesigns of RO systems such as the incorporation of a second pass, etc. Gao et al. (2011). Another additional factor that may affect boron rejection in SWRO systems is membrane fouling. This can be appreciated in the study published by Ruiz-García et al. (2019) in which two commercial SWRO membranes were evaluated in a full-scale desalination plant. Park et al. (2012) evaluated the decrease of boron removal and the reduction in the water production rate by membrane fouling. The study was based on simulations and a predictive model that estimates boron removal in SWRO desalination processes was used.

The intensive use of energy in SWRO desalination plants has promoted the use of renewable energy sources (RES) to provide the power for this technology (Nassrullah et al., 2020). The application of RES to power SWRO is not simple, and its viability depends on many factors such as water and energy accessibility (Nassrullah et al., 2020), costs (Elmaadawy et al., 2020; Rezk et al., 2020), regulations (Sen and Ganguly, 2017), etc. There are two main factors in the operation of an SWRO desalination plant, permeate production and permeate quality in terms of total dissolved solids (TDS). Both factors are affected when an off-grid RES is powering the SWRO system under variable conditions. de la Nuez Pestana et al. (2004) studied the variable operation of an SWRO system directly connected to a wind turbine without any energy storage system. The membrane installed in this SWRO system was the TFC 2822-SS from Koch Fluid Systems™, and actual seawater (as opposed to synthesized) was used. The feed pressures (p_f) applied were 39, 49 and 60 bar, with flux recoveries of 19.74, 31.37 and 40% respectively. Permeate conductivity was between 429 and 292 μS cm^{-1}, with lower values at pressures of 49 and 60 bar. Ntavou et al. (2016) carried out a performance analysis of a multi-skid SWRO unit under variable power input. They used a FILMTEC™SW30-4040 membrane and a synthesized feed solution by adding salt to tap water to reach 37,500 ppm. It was observed that the lower the TDS in the permeate (TDS_p) the higher the power input that was required, with TDS_p ranging between approximately 150 and 250 ppm. Dimitriou et al. (2017) validated a theoretical model for predicting SWRO systems under variable operating conditions. As in the previous study, the membrane used was the FILMTEC™SW30-4040 in a small-scale SWRO unit with one pressure vessel (PV) and a Clark pump unit. p_f ranged between 35 and 45 bar approximately and TDS_p between 200 and 600 ppm. They also obtained lower TDS_p with higher p_f. The same SWRO system was used by C.-S. Karavas et al. (2018), incorporating a short-term energy storage system. In this case, they operated the SWRO system in a p_f range of between 39 and 51 bar, with a permeate conductivity of between 200 and 1000 μS cm^{-1}. As is usual in these desalination systems, the higher the power input was, the higher the pressure and R and the lower the TDS_p were. Calise et al. (2019) carried out an economic assessment study of SWRO desalination powered by photovoltaic panels. The performance analysis of the SWRO system was based on a simulation using the Water Application Value Engine (WAVE) software from Dupont® and a model proposed by the authors which showed similar results. The performance was assessed in terms of R and salt rejection. An off-grid solar energy system to power an SWRO desalination plant with integrated photovoltaic thermal cooling was proposed by Monjezi et al. (2020). The modeling and operation of the SWRO system was simulated with the Reverse Osmosis System Analysis (ROSA) software. The authors studied the Filmtec™SW30-2540 membrane, working with a single stage

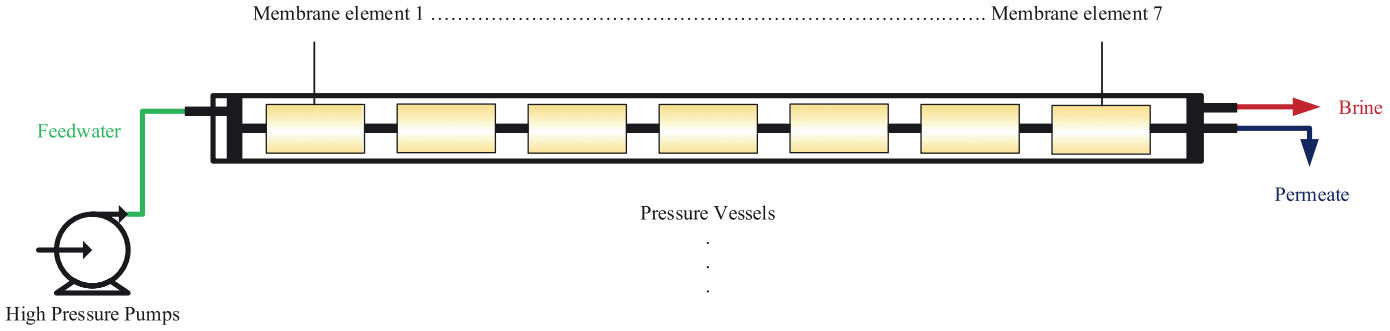

Fig. 1. Flow diagram of the SWRO system.

with an R of 40%. An inorganic feedwater was used as input, but boron concentration was non-existent and the concentration of each ion in the permeate was estimated by the software. Delgado-Torres et al. (2020) undertook a preliminary study of an SWRO process powered by a hybrid system (photovoltaic - tidal range). The performance of the SWRO system was simulated with ROSA, considering two SWRO membranes: FILMTEC^{TM}SW30HRLE - 440i and FILMTEC^{TM}SW30XLE - 440i. The inorganic composition of the feedwater was not detailed and only the TDS_p of one operating point for each membrane was shown. Unfortunately, the issue of boron rejection in SWRO systems working under variable operating conditions has not been extensively studied. The permitted permeate boron concentrations according to different regulations are low. While the World Health Organization (WHO) established a maximum boron concentration of 2.4 ppm for drinking water in 2011, the EU limit is just 1.0 ppm. This limiting factor can reduce the safe operation windows (SOWs) of SWRO systems working under variable input power as supplied by RES.

The aim and novel contribution of this paper is the evaluation of the performance and the boron rejection under variable operating conditions of two commercial SWRO membranes (TM820L-440 and TM820S-400 from Toray) in full-scale PVs. To carry out this work, a simulation algorithm previously validated and published by the authors Ruiz-García and de la Nuez-Pestana (2018) was adapted to estimate the behavior of a single-stage SWRO system with the aforementioned membranes installed. The permeability coefficients of RO membranes are characteristic to each membrane and show membrane efficiency in terms of water production and solute rejection. The initial average water, salt and boron permeability coefficients that were used were taken from a previous published work (Ruiz-García et al., 2019).

2. Material and methods

2.1. Permeability coefficients

Determination of the initial water permeability coefficient (A), salt permeability coefficient (B_s) and B_B was carried out using the experimental data of the initial operating point of a full-scale SWRO desalination plant with TM820L-440 and TM820S-400 membranes installed. A more detailed description of this desalination plant can be found in a previous work published by one of the authors Ruiz-García et al. (2019). More specifically, the initial data of trains 2 (TM820L-440) and 9 (TM820S-400) were used. These trains were selected as their initial operating time was closer to 0 than the other trains and so their membranes were the least used. The number of PVs was 90 and 79 for trains 2 and 9, respectively. Each PV had 7 SWRO membrane elements in series (Fig. 1). As the operating data were usually collected at the input and output of the PVs, this allowed calculation of the average permeability coefficients. The detailed procedure for calculating the permeability coefficient can be found in a previous study by Ruiz-García et al. (2019). Conductivity was measured using a Hanna® Instruments EC 215 conductivity meter, and boron concentration in the permeate was determined using the carmine method. The pH was close to 7, so B_B was calculated as boric acid. The permeability coefficients per SWRO membrane module were estimated from the initial operating data. Table 1 show the dimensional characteristics and performance under manufacturer test conditions (p_f=5.52 MPa, feed-brine temperature (T_{fb}) =25 °C, C_f=32,000 ppm NaCl, R=8%, pH_p=8 and 5 ppm boron added to feedwater) of the SWRO membranes and Table 2 shows the initial operating values per PV and the permeability coefficients for each membrane. For these calculation the Equations of Table 3 were used.

Table 1
Dimensional characteristics of membrane elements and performance under manufacturer test conditions.

Parameters	TM820L-440	TM820S-400
Manufacturer	Toray	Toray
Configuration	Spiral wound	Spiral wound
Area (m^2)	40.88	37.16
Length (m)	1.016	1.016
Diameter (m)	0.2	0.2
Feed-brine spacer height (m)	7.11×10^{-4}	7.11×10^{-4}
Permeate flow (Q_p) (m^3 h^{-1})	2.13	1.42
Salt rejection (%)	99.8	99.75
Boron rejection (%)	90	92

2.2. Process modeling

The simulation algorithm (Ruiz-García and de la Nuez-Pestana, 2018) used the solution-diffusion (Qasim et al., 2019; Al-Obaidi et al., 2017) transport model. This is the most commonly used model for simulating (Joseph and Damodaran, 2019) and predicting RO system performances (Alsarayreh et al., 2020a; Al-Obaidi et al., 2019) as usually provides results close to the real behavior of these systems, despite its limitations (Alsarayreh et al., 2020b). The transport equations are applied for each membrane element considering averages. The temperature T and pressure drop in the permeate along the RO system were disregarded. More details about the simulation algorithm can be found in a previous work (Ruiz-García and de la Nuez-Pestana, 2018). A fouling factor (FF) of 1 was considered (new membrane) along with a T_{fb} of 25 °C, and so the temperature correction factor (TCF) was 1. S_m is the active membrane surface, NDP the net driving pressure, L the membrane length, v_{fb} the feed-brine velocity, ε the porosity in the feed-brine channel (considered 0.89 for both membranes), h the feed-brine spacer height (28 milli-inches= 7.11×10^{-4} m), PF the polarization factor, k_s the solute mass transfer coefficient and η the dynamic viscosity of water (0.000891 kg m^{-1} s^{-1}). To determine all the above variables, the aforementioned algorithm was imple-

Table 2
Operating parameters and SWRO membrane permeability coefficients.

Parameters	TM820L-440	TM820S-400
Feed flow (Q_f) ($m^3\ h^{-1}$)	8.53	9.7
Feed pressure (p_f) (MPa)	6.7	6.45
Permeate flow (Q_p) ($m^3\ h^{-1}$)	3.83	4.28
Permeate concentration (C_p) (ppm)	251.44	240.8
Boron concentration in the permeate (C_{pB}) (ppm)	0.6	0.89
Initial average water permeability coefficient (A_{av}) ($m\ Pa^{-1}s^{-1}$)	1.24×10^{-12}	2.01×10^{-12}
Initial average solute permeability coefficient (B_{av-s}) ($m\ s^{-1}$)	1.76×10^{-8}	2.20×10^{-8}
Initial average boron permeability coefficient (B_{av-B}) ($m\ s^{-1}$)	3.55×10^{-7}	7.31×10^{-7}
Initial A (A) ($m\ Pa^{-1}s^{-1}$)	1.85×10^{-12}	2.65×10^{-12}
Initial B_s ($m\ s^{-1}$)	1.55×10^{-8}	1.75×10^{-8}
Initial B_B ($m\ s^{-1}$)	3.15×10^{-7}	5.65×10^{-7}

Table 3
Transport equations.

Permeate flow	$Q_p = A \cdot NDP \cdot S_m$	(1)
Water permeability coefficient	$A = A_0 \cdot TCF \cdot FF$	(2)
Net driving pressure	$NDP = (\Delta p - \Delta\pi) = p_f - \frac{\Delta p_{fb}}{2} - p_p - \pi_m + \pi_p$	(3)
Feed-brine pressure drop	$\Delta p_{fb} = \lambda \cdot L \cdot \frac{\rho_{fb}}{d_h} \frac{v_{fb}}{2}$	(4)
Friction factor	$\lambda = 2.3Re^{-0.31}$	(5)
Reynolds number	$Re = \frac{\rho_{fb} \cdot v_{fb} \cdot d_h}{\eta}$	(6)
Hydraulic diameter	$d_h = \frac{4\varepsilon}{\frac{2}{h} + (1-\varepsilon)\frac{8}{h}}$	(7)
Seawater density	$\rho_{fb} = 498.4 \cdot M + \sqrt{248400 + 752.4 \cdot C_{fb} \cdot M}$	(8)
Empirical parameter	$M = 1.0069 - 2.757 \times 10^{-4} \cdot T_{fb}$	(9)
Feed-brine concentration	$C_{fb} = C_f \cdot \left(\frac{1 + \frac{C_b}{C_f}}{2}\right)$	(10)
Osmotic pressure	$\pi = 4.54047 \cdot \left(10^3 \cdot C/(M_s \cdot \rho)\right)^{0.987}$	(11)
Concentration on membrane surface	$C_m = C_{fb} \cdot PF$	(12)
Polarization factor	$PF = \frac{C_m}{C_{fb}} = e^{\frac{J_p}{k}}$	(13)
Shearwood number	$Sh = 0.14 \cdot Re^{0.64} \cdot Sc^{0.42} = \frac{k \cdot d_h}{D_s}$	(14)
Schmidt number	$Sc = \frac{\eta}{\rho_{fb} \cdot D_s}$	(15)
Boron mass transfer coefficient (Taniguchi et al., 2001)	$k_B = 0.97 \cdot k_s$	(16)
Solute diffusivity	$D_s = (0.72598 + 0.023087T_{fb} + 0.00027657T_{fb}^2) \times 10^{-9}$	(17)
Permeate concentration	$C_p = B \cdot PF \cdot TCF \cdot \frac{S_m}{Q_p} \cdot \left(\frac{C_f \cdot (1+CF)}{2}\right)$	(18)
Concentration factor	$CF = \frac{100}{100-R}$	(19)
Flux recovery	$R = 100 \cdot \frac{Q_p}{Q_f}$	(20)
Rejection	$Rejection = 100 - \frac{C_p}{C_m}$	(21)

mented in MATLAB®. The results are presented per PV of 7 membrane elements each (as in the actual SWRO system). The simulations were carried out with the following operating ranges per PV: Q_f from 5 to 16 $m^3\ h^{-1}$ since for Q_f between 3 and 5 $m^3\ h^{-1}$ the operating window was small and with low R, C_f from 32 to 45 g L^{-1} and p_f from 4 to 7 MPa. Boron concentration in the feedwater was considered as 5 ppm in all cases in accordance with the analysis of the feedwater carried out in the desalination plant (Ruiz-García et al., 2019). Only NaCl was increased. The specific energy consumption (SEC) was determined considering the ideal performance of the high pressure pump (100% efficiency for the electrical engine and pump). No energy recovery devices were considered in the simulations.

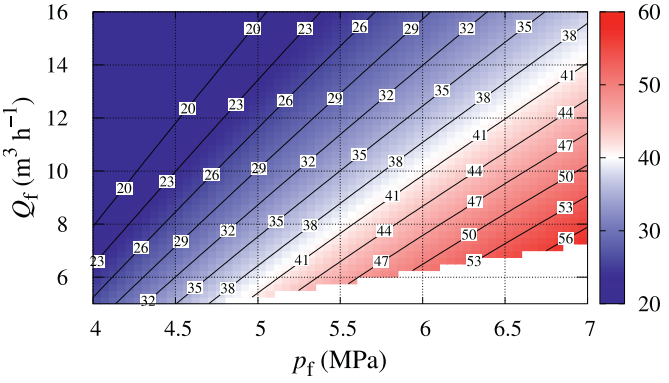

Fig. 2. R (%) of the membranes TM820L-440.

3. Results and discussion

The results shown in Figs. 2–9 were obtained considering C_f=35,000 ppm. Figs. 2 and 3 show the R of the TM820L-440 and TM820S-400 membranes, respectively. It can be observed that higher R was achieved with the TM820S-440 membrane for the same operating points. The influence of coefficient A was higher than the active area of the membranes in terms of R. High R values can bring some membrane elements close to thresholds imposed by manufacturers including, for example, R higher than 15% per element or brine flow rates (Q_b) very close to 3 $m\ h^{-3}$. Such operating conditions can decrease notably the system performance over long periods of operation and mean that more frequent chemical cleanings are required, etc. The highest R values obtained were 57.56 and 58.45% for the TM820L-440 (7 MPa, 7.25 $m^3\ h^{-1}$) and TM820S-400 (7 MPa, 8.5 $m^3\ h^{-1}$) membranes, respectively.

Figs. 4 and 5 show the SEC values of the TM820L-440 and TM820S-400 membranes, respectively. As usual, the membrane with higher R had the lower SEC. The TM820L-440 membrane had a larger SOW, mainly due to the A coefficient. This membrane had lower production, and so there were more operating points where restrictions such as minimum Q_b or maximum R per membrane element were not reached. For this reason, depending on the operating conditions, it is not advisable to have many high production membrane elements in series. Minimum values of SEC were 3.12

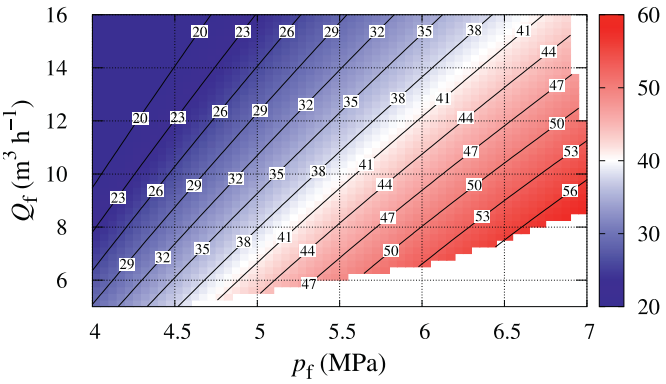

Fig. 3. *R* (%) of the membranes TM820S-400.

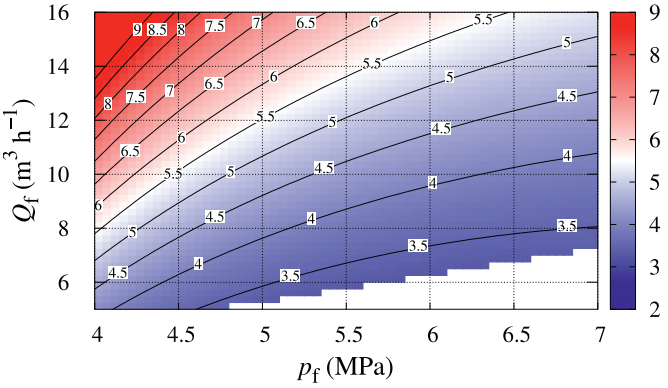

Fig. 4. *SEC* (kWh m^{-3}) of the membranes TM820L-440.

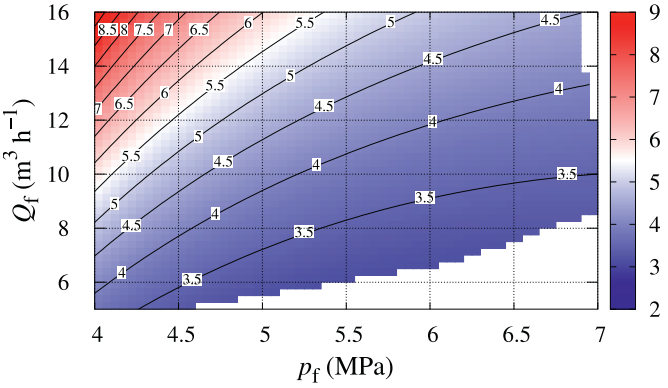

Fig. 5. *SEC* (kWh m^{-3}) of the membranes TM820S-400.

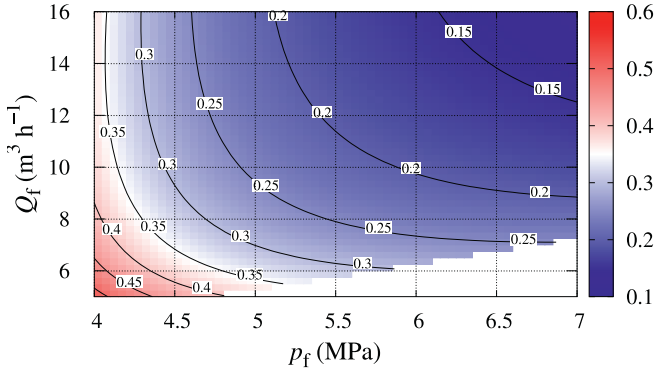

Fig. 6. $C_p \times 10^{-3}$ (ppm) of the membrane TM820L-440.

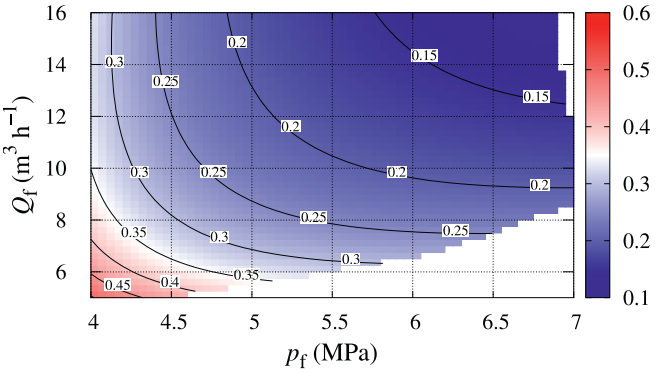

Fig. 7. $C_p \times 10^{-3}$ (ppm) of the membrane TM820S-400.

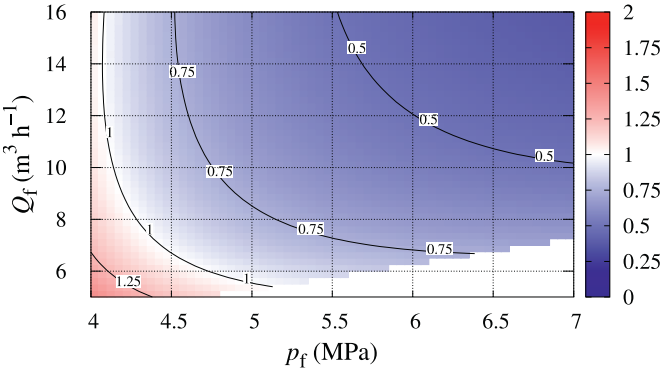

Fig. 8. C_{pB} (ppm) of the membrane TM820L-440.

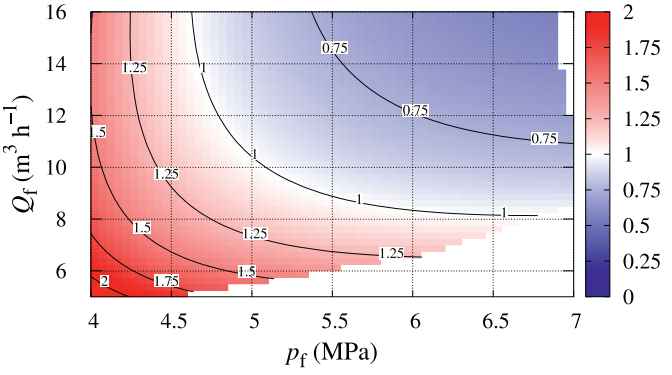

Fig. 9. C_{pB} (ppm) of the membrane TM820S-400.

and 3.27 kWh m^{-3} for membranes TM820S-400 and TM820L-440 respectively (considering ideal performance). Usually these operating points are very close to the thresholds imposed by manufacturers and it is convenient to take safety margins in real operation. The lowest *SEC* values obtained were 3.2683 and 3.1180 kWh m^{-3} for the TM820L-440 (5.85 MPa, 6 m^3 h $^{-1}$) and TM820S-400 (5.55 MPa, 6 m^3 h $^{-1}$) membranes, respectively.

For both membranes, the higher Q_f and p_f were the lower C_p was (Figs. 6 and 7). The higher Q_p and the lower *CF* were, the lower C_p was. (Eq. (17)). High values of Q_p required high values of Q_f and p_f. The mentioned two figures show the role of coefficient *B* in solute rejection. The difference is very small as the coefficients are quite close (1.55×10^{-8} vs 1.75×10^{-8}). It should be considered that fouling could have a different impact on both membranes making the coefficient *B* vary differently. However, the difference between the two membranes in terms of B_B was more pronounced. This can be observed in Figs. 8 and 9, which show

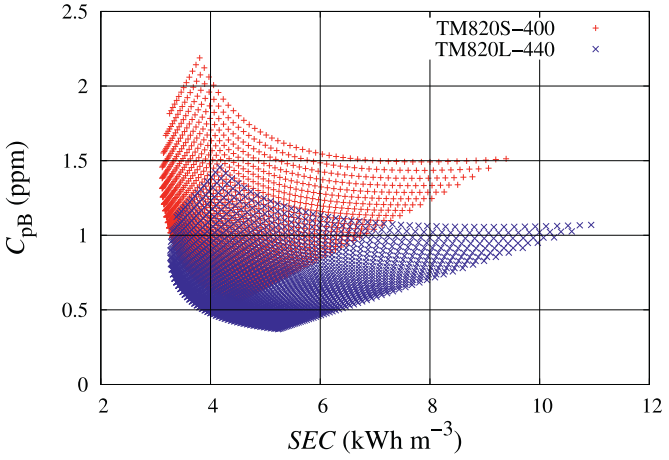

Fig. 10. *SEC* vs C_{pB} of the membranes TM820L-440 and TM820S-400.

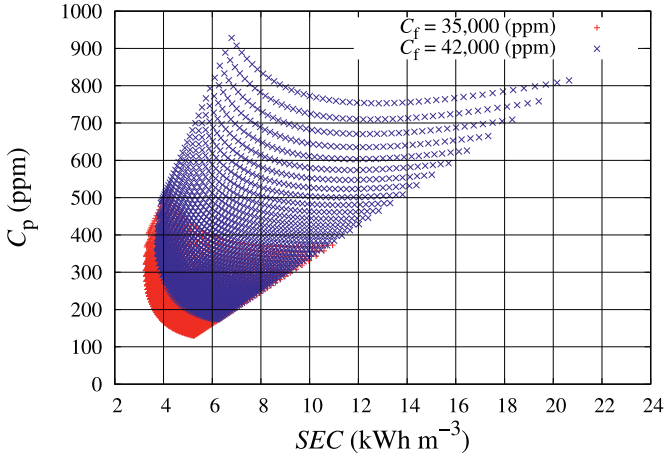

Fig. 11. *SEC* vs C_p of the membrane TM820L-440 considering C_f of 35,000 and 42,000 ppm.

boron concentration in the permeate. The TM820L-440 membrane was able to maintain lower C_{pB} in a wider operating range, making it more suitable than the TM820S-400 in terms of boron rejection as boric acid, although the energy requirements were higher. For this reason, two types of SWRO membranes (one with high boron rejection and another with high production) are installed in some SWRO desalination plants in order to balance the *SEC* and C_{pB} (Ruiz-García et al., 2019). If the SWRO system is working under variable operation this task becomes much more complex, this is why to have a SOW is crucial.

Fig. 10 shows the *SEC* vs C_{pB} for the two membranes. Considering a limiting factor of 1 ppm for C_{pB}, it can be seen that the TM820L-440 membrane had a wider operating window that allowed an appropriate C_{pB}. While there were various operating points that could allow the same C_{pB}, the actual operating point of the SWRO system will depend on the high pressure pump installed. Fig. 11 shows the displacement of the SOW of the TM820L-440 membrane considering two different C_f (35 and 42,000 ppm). It can be seen how the SOW for the higher C_f was wider. This was due to higher osmotic pressure resulting in the SWRO membrane element produce less permeate under the same operating conditions and lower C_f. This decrease in production meant the SWRO membrane did not exceed the safety operation margin for most operating points, although many operating points showed an unacceptable C_p and high *SEC*. It should be noted that all the results were obtained considering constant permeability coefficients. In actual operation, fouling can cause the permeability coefficients to change (Ruiz-García and Nuez, 2020), in which case all the possible operating points would be displaced with respect to the calculated ones. A decrease in coefficient *A* can produce decreases in *R* and/or increases in *SEC* if a constant *R* is desired by increasing p_f. A change in coefficient B_B could be delicate as it may result in the need for changes in the operating conditions to ensure the quality criteria are met, as well as, in some cases, premature membrane replacement.

4. Conclusions

An evaluation was undertaken in this work of boron rejection (in the form of boric acid) of two commercial membranes (TM820L-440 and TM820S-400) under variable operating conditions. The results show that the TM820L-440 membrane is the more suitable option in SWRO systems where the required C_{pB} is low (< 1 ppm) and a priority. However, as the TM820L-440 requires more energy than the TM820S-400, the latter is more appropriate when C_{pB} is not a priority or when the limiting concentration is not very low, such as for agricultural purposes (non boron-sensitive crops). It should be noted that this was a static study (constant permeability coefficient) and that in SWRO systems the permeability coefficient is usually not constant, mainly due to the effect of fouling on the system. This can produce important variations in performance and may require changes to the operating conditions. Works on the sizing and techno-economic assessment of RES-powered SWRO systems should take into account not only the SOW, considering new membranes or constant permeability coefficients, but also the change of these coefficients and its impact on the entire plant. The decrease in coefficient *A* could result in lower permeate production or the need to oversize the RES system to provide the energy required to ensure constant long-term permeate production. Future works should consider different permeability coefficients under variable operating conditions to enable the determination of the most suitable membranes in terms of performance in certain operating ranges.

Declaration of Competing Interest

The authors declare that they have no known competing financial interests or personal relationships that could have appeared to influence the work reported in this paper.

CRediT authorship contribution statement

A. Ruiz-García: Conceptualization, Methodology, Data curation, Writing - original draft, Visualization, Investigation, Validation, Writing - review & editing. **I. Nuez:** Conceptualization, Resources, Supervision.

Acknowledgement

This research has been co-funded with ERDF funds, the INTERREG V-A MAC 2014–2020 program, ACLIEMAC Project (MAC2/3.5b/380).

References

Al-Obaidi, M., Kara-Zaïtri, C., Mujtaba, I., 2019. Evaluation of chlorophenol removal from wastewater using multi-stage spiral-wound reverse osmosis process via simulation. Comput. Chem. Eng. 130, 106522. doi:10.1016/j.compchemeng.2019.106522. https://www.sciencedirect.com/science/article/pii/S0098135418310408

Alkhudhiri, A., Bin Darwish, N., Hakami, M.W., Abdullah, A., Alsadun, A., Abu Homod, H., 2020. Boron removal by membrane distillation: a comparison study. Membranes 10 (10), 1–15. doi:10.3390/membranes10100263. https://www.mdpi.com/2077-0375/10/10/263

Alsarayreh, A.A., Al-Obaidi, M., Al-Hroub, A., Patel, R., Mujtaba, I., 2020. Performance evaluation of reverse osmosis brackish water desalination plant with different recycled ratios of retentate. Comput. Chem. Eng. 135, 106729. doi:10.1016/j.compchemeng.2020.106729. https://www.sciencedirect.com/science/article/pii/S0098135419310348

Alsarayreh, A.A., Al-Obaidi, M.A., Patel, R., Mujtaba, I.M., 2020. Scope and limitations of modelling, simulation, and optimisation of a spiral wound reverse osmosis process-based water desalination. Processes 8 (5), 1–31. doi:10.3390/pr8050573. https://www.mdpi.com/2227-9717/8/5/573

Ban, S.-H., Im, S.-J., Cho, J., Jang, A., 2019. Comparative performance of FO-RO hybrid and two-pass SWRO desalination processes: boron removal. Desalination 471, 114114. doi:10.1016/j.desal.2019.114114. http://www.sciencedirect.com/science/article/pii/S0011916419313931

Calise, F., Cappiello, F.L., Vanoli, R., Vicidomini, M., 2019. Economic assessment of renewable energy systems integrating photovoltaic panels, seawater desalination and water storage. Appl. Energy 253, 113575. doi:10.1016/j.apenergy.2019.113575. http://www.sciencedirect.com/science/article/pii/S0306261919312498

Cengeloglu, Y., Arslan, G., Tor, A., Kocak, I., Dursun, N., 2008. Removal of boron from water by using reverse osmosis. Sep. Purif. Technol. 64 (2), 141–146. doi:10.1016/j.seppur.2008.09.006.

Chen, M., Dollar, O., Shafer-Peltier, K., Randtke, S., Waseem, S., Peltier, E., 2020. Boron removal by electrocoagulation: removal mechanism, adsorption models and factors influencing removal. Water Res. 170, 115362. doi:10.1016/j.watres.2019.115362. http://www.sciencedirect.com/science/article/pii/S0043135419311364

Darwish, N.B., Alkhudhiri, A., AlAlawi, A., AlRomaih, H., Hilal, N., 2020. Experimental investigation of forward osmosis process for boron removal from water. J. Water Process Eng. 38, 101570. doi:10.1016/j.jwpe.2020.101570. http://www.sciencedirect.com/science/article/pii/S2214714420304487

Darwish, N.B., Kochkodan, V., Hilal, N., 2017. Microfiltration of micro-sized suspensions of boron-selective resin with PVDF membranes. Desalination 403, 161–171. doi:10.1016/j.desal.2016.04.018. Desalination Using Membrane Technology

de la Nuez Pestana, I., Javier García Latorre, F., Argudo Espinoza, C., Gómez Gotor, A., 2004. Optimization of RO desalination systems powered by renewable energies. Part I: wind energy. Desalination 160 (3), 293–299. doi:10.1016/S0011-9164(04)90031-8. http://www.sciencedirect.com/science/article/pii/S0011916404900318

Delgado-Torres, A.M., García-Rodríguez, L., del Moral, M.J., 2020. Preliminary assessment of innovative seawater reverse osmosis (SWRO) desalination powered by a hybrid solar photovoltaic (PV) - tidal range energy system. Desalination 477, 114247. doi:10.1016/j.desal.2019.114247. https://www.sciencedirect.com/science/article/pii/S0011916419313529

Dimitriou, E., Boutikos, P., Mohamed, E.S., Koziel, S., Papadakis, G., 2017. Theoretical performance prediction of a reverse osmosis desalination membrane element under variable operating conditions. Desalination 419, 70–78. doi:10.1016/j.desal.2017.06.001. http://www.sciencedirect.com/science/article/pii/S0011916416318847

Elmaadawy, K., Kotb, K.M., Elkadeem, M., Sharshir, S.W., Dán, A., Moawad, A., Liu, B., 2020. Optimal sizing and techno-enviro-economic feasibility assessment of large-scale reverse osmosis desalination powered with hybrid renewable energy sources. Energy Convers. Manag. 224, 113377. doi:10.1016/j.enconman.2020.113377. http://www.sciencedirect.com/science/article/pii/S0196890420309146

Farhat, A., Ahmad, F., Arafat, H., 2013. Analytical techniques for boron quantification supporting desalination processes: a review. Desalination 310, 9–17. doi:10.1016/j.desal.2011.12.020. Removal of Boron from Seawater, Geothermal Water and Wastewater

Gao, D., Guo, Y., Wang, S., Deng, T., 2011. Boron removal from seawater desalination by RO. In: 2011 International Conference on Consumer Electronics, Communications and Networks (CECNet), pp. 4825–4828. doi:10.1109/CECNET.2011.5768445.

Glueckstern, P., Priel, M., 2003. Optimization of boron removal in old and new SWRO systems. Desalination 156 (1), 219–228. doi:10.1016/S0011-9164(03)00344-8. Joint EDS, WSTA and IWA conference on Desalination and the Environment Fresh Water for All UN International Year of Fresh Water 2003

Hasson, D., Shemer, H., Brook, I., Zaslavschi, I., Semiat, R., Bartels, C., Wilf, M., 2011. Scaling propensity of seawater in RO boron removal processes. J. Membr. Sci. 384 (1), 198–204. doi:10.1016/j.memsci.2011.09.027. https://www.sciencedirect.com/science/article/pii/S0376738811006983

Hilal, N., Kim, G., Somerfield, C., 2011. Boron removal from saline water: a comprehensive review. Desalination 273 (1), 23–35. doi:10.1016/j.desal.2010.05.012. Special issue to mark the 45th Anniversary of launching Desalination journal and to honour Professor David Hasson for his enormous support and contribution to Desalination

Hussain, A., Sharma, R., Minier-Matar, J., Hirani, Z., Adham, S., 2019. Application of emerging ion exchange resin for boron removal from saline groundwater. J. Water Process Eng. 32, 100906. doi:10.1016/j.jwpe.2019.100906. http://www.sciencedirect.com/science/article/pii/S2214714419303769

Hyung, H., Kim, J.-H., 2006. A mechanistic study on boron rejection by sea water reverse osmosis membranes. J. Membr. Sci. 286 (1), 269–278. doi:10.1016/j.memsci.2006.09.043. http://www.sciencedirect.com/science/article/pii/S0376738806006569

Jarma, Y.A., Çermikli, E., Ipekçi, D., Altıok, E., Kabay, N., 2021. Comparison of two electrodialysis stacks having different ion exchange and bipolar membranes for simultaneous separation of boron and lithium from aqueous solution. Desalination 500, 114850. doi:10.1016/j.desal.2020.114850. http://www.sciencedirect.com/science/article/pii/S0011916420315289

Jiang, B., Zhang, X., Zhao, X., Li, F., 2018. Removal of high level boron in aqueous solutions using continuous electrodeionization (CEDI). Sep. Purif. Technol. 192, 297–301. doi:10.1016/j.seppur.2017.10.012. http://www.sciencedirect.com/science/article/pii/S1383586617315812

Joseph, A., Damodaran, V., 2019. Dynamic simulation of the reverse osmosis process for seawater using LabVIEW and an analysis of the process performance. Comput. Chem. Eng. 121, 294–305. doi:10.1016/j.compchemeng.2018.11.001. https://www.sciencedirect.com/science/article/pii/S0098135418307385

Jung, B., Kim, C.Y., Jiao, S., Rao, U., Dudchenko, A.V., Tester, J., Jassby, D., 2020. Enhancing boron rejection on electrically conducting reverse osmosis membranes through local electrochemical ph modification. Desalination 476, 114212. doi:10.1016/j.desal.2019.114212. http://www.sciencedirect.com/science/article/pii/S0011916419317837

Karavas, C.-S., Arvanitis, K.G., Kyriakarakos, G., Piromalis, D.D., Papadakis, G., 2018. A novel autonomous PV powered desalination system based on a DC microgrid concept incorporating short-term energy storage. Sol. Energy 159, 947–961. doi:10.1016/j.solener.2017.11.057. http://www.sciencedirect.com/science/article/pii/S0038092X17310502

Kluczka, J., Pudło, W., Krukiewicz, K., 2019. Boron adsorption removal by commercial and modified activated carbons. Chem. Eng. Res. Des. 147, 30–42. doi:10.1016/j.cherd.2019.04.021. http://www.sciencedirect.com/science/article/pii/S0263876219301790

Koseoglu, H., Kabay, N., Yüksel, M., Kitis, M., 2008. The removal of boron from model solutions and seawater using reverse osmosis membranes. Desalination 223 (1), 126–133. doi:10.1016/j.desal.2007.01.189. European Desalination Society and Center for Research and Technology Hellas (CERTH), Sani Resort 22–25 April 2007, Halkidiki, Greece

Koseoglu, H., Kabay, N., Yüksel, M., Sarp, S., Arar, Ö., Kitis, M., 2008. Boron removal from seawater using high rejection SWRO membranes impact of pH, feed concentration, pressure, and cross-flow velocity. Desalination 227 (1), 253–263. doi:10.1016/j.desal.2007.06.029.

Li, Y., Wang, S., Song, X., Zhou, Y., Shen, H., Cao, X., Zhang, P., Gao, C., 2020. High boron removal polyamide reverse osmosis membranes by swelling induced embedding of a sulfonyl molecular plug. J. Membr. Sci. 597, 117716. doi:10.1016/j.memsci.2019.117716. http://www.sciencedirect.com/science/article/pii/S0376738819328625

Al-Obaidi, M.A., Kara-Zaitri, C., I.M. Mujtaba, 2017. Scope and limitations of the irreversible thermodynamics and the solution diffusion models for the separation of binary and multi-component systems in reverse osmosis process. Comput. Chem. Eng. 100, 48–79. doi:10.1016/j.compchemeng.2017.02.001. http://www.sciencedirect.com/science/article/pii/S0098135417300571

Monjezi, A.A., Chen, Y., Vepa, R., Kashyout, A.E.-H.B., Hassan, G., Fath, H.E.-B., Kassem, A.E.-W., Shaheed, M.H., 2020. Development of an off-grid solar energy powered reverse osmosis desalination system for continuous production of freshwater with integrated photovoltaic thermal (PVT) cooling. Desalination 495, 114679. doi:10.1016/j.desal.2020.114679. http://www.sciencedirect.com/science/article/pii/S0011916420313576

Najid, N., Kouzbour, S., Ruiz-García, A., Fellaou, S., Gourich, B., Stiriba, Y., 2021. Comparison analysis of different technologies for the removal of boron from seawater: a review. J. Environ. Chem. Eng. 105133. doi:10.1016/j.jece.2021.105133. http://www.sciencedirect.com/science/article/pii/S2213343721001111

Nassrullah, H., Anis, S.F., Hashaikeh, R., Hilal, N., 2020. Energy for desalination: a state-of-the-art review. Desalination 491, 114569. doi:10.1016/j.desal.2020.114569. http://www.sciencedirect.com/science/article/pii/S0011916420310304

Neo, J.G., Japip, S., Luo, L., Chung, T.-S., Weber, M., Maletzko, C., 2019. Hydroxyl-terminated poly(ethyleneimine) polymer enhanced ultrafiltration for boron removal. Sep. Purif. Technol. 222, 214–220. doi:10.1016/j.seppur.2019.04.006. http://www.sciencedirect.com/science/article/pii/S1383586619304228

Ntavou, E., Kosmadakis, G., Manolakos, D., Papadakis, G., Papantonis, D., 2016. Experimental evaluation of a multi-skid reverse osmosis unit operating at fluctuating power input. Desalination 398, 77–86. doi:10.1016/j.desal.2016.07.014. http://www.sciencedirect.com/science/article/pii/S0011916416308451

Ozbey-Unal, B., Imer, D.Y., Keskinler, B., Koyuncu, I., 2018. Boron removal from geothermal water by air gap membrane distillation. Desalination 433, 141–150. doi:10.1016/j.desal.2018.01.033. http://www.sciencedirect.com/science/article/pii/S001191641732372X

Park, P.-K., Lee, S., Cho, J.-S., Kim, J.-H., 2012. Full-scale simulation of seawater reverse osmosis desalination processes for boron removal: effect of membrane fouling. Water Res. 46 (12), 3796–3804. doi:10.1016/j.watres.2012.04.021. https://www.sciencedirect.com/science/article/pii/S004313541200276X

Qasim, M., Badrelzaman, M., Darwish, N.N., Darwish, N.A., Hilal, N., 2019. Reverse osmosis desalination: a state-of-the-art review. Desalination 459, 59–104. doi:10.1016/j.desal.2019.02.008. http://www.sciencedirect.com/science/article/pii/S0011916418325037

Rezk, H., Alghassab, M., Ziedan, H.A., 2020. An optimal sizing of stand-alone hybrid PV-fuel cell-battery to desalinate seawater at Saudi NEOM city. Processes 8 (4), 1–19. doi:10.3390/pr8040382. https://www.mdpi.com/2227-9717/8/4/382

Ruiz-García, A., León, F., Ramos-Martín, A., 2019. Different boron rejection behavior in two RO membranes installed in the same full-scale SWRO desalination plant. Desalination 449, 131–138. doi:10.1016/j.desal.2018.07.012. http://www.sciencedirect.com/science/article/pii/S001191641830609X

Ruiz-García, A., Nuez, I., 2020. Long-term intermittent operation of a full-scale BWRO desalination plant. Desalination 489, 114526. doi:10.1016/j.desal.2020.114526. http://www.sciencedirect.com/science/article/pii/S0011916420305403

Ruiz-García, A., Nuez, I., Carrascosa-Chisvert, M., Santana, J., 2020. Simulations of BWRO systems under different feedwater characteristics. analysis of op-

eration windows and optimal operating points. Desalination 491, 114582. doi:10.1016/j.desal.2020.114582. https://www.sciencedirect.com/science/article/pii/S0011916420307207

Ruiz-García, A., de la Nuez-Pestana, I., 2018. A computational tool for designing BWRO systems with spiral wound modules. Desalination 426, 69–77. doi:10.1016/j.desal.2017.10.040. http://www.sciencedirect.com/science/article/pii/S0011916417310950

Sagiv, A., Semiat, R., 2004. Analysis of parameters affecting boron permeation through reverse osmosis membranes. J. Membr. Sci. 243 (1), 79–87. doi:10.1016/j.memsci.2004.05.029. http://www.sciencedirect.com/science/article/pii/S0376738804004132

Sen, S., Ganguly, S., 2017. Opportunities, barriers and issues with renewable energy development - a discussion. Renew. Sust. Energ. Rev. 69, 1170–1181. doi:10.1016/j.rser.2016.09.137. http://www.sciencedirect.com/science/article/pii/S1364032116306487

Taniguchi, M., Kurihara, M., Kimura, S., 2001. Boron reduction performance of reverse osmosis seawater desalination process. J. Membr. Sci. 183 (2), 259–267. doi:10.1016/S0376-7388(00)00596-2. http://www.sciencedirect.com/science/article/pii/S0376738800005962

Wang, S., Zhou, Y., Gao, C., 2018. Novel high boron removal polyamide reverse osmosis membranes. J. Membr. Sci. 554, 244–252. doi:10.1016/j.memsci.2018.03.014. http://www.sciencedirect.com/science/article/pii/S0376738817331587

Wolska, J., Bryjak, M., 2013. Methods for boron removal from aqueous solutions-areview. Desalination 310, 18–24. doi:10.1016/j.desal.2012.08.003. Removal of Boron from Seawater, Geothermal Water and Wastewater